Energy Equip. Sys./ Vol. 14/No. 1/March 2026/ 33-56

ENERGY EQUIPSYS

Energy Equipment and Systems

www.energyequipsys.com

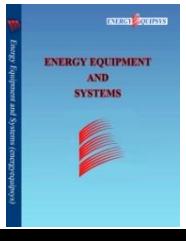

Performance analysis of solar assisted thermal power cycle in integration with thermal storage systems

Manuscript Type
Research Paper

Authors

Khandelwal Neelam [a]
Sharma Meeta[b*]
Shukla Anoop Kumar[b]

[a] JSS Academy of Technical Education, Noida (U.P.), India

[b] Amity University Uttar Pradesh, Noida (U.P.), India

Article history:
Received: 4 March 2025
Revised: 16 August 2025
Accepted : 26 October 2025

ABSTRACT

Thermal power plants are facing issues such as fuel depletion, CO2 emissions, and ash handling, among others. The integration of a concentrated solar (CS) system with the existing power cycle is the way to minimize these issues. The CSPP has the issue of energy differential between its demand and the intermittent availability of solar energy. The integration of Thermal Energy Storage (TES) with these plants can address the issues associated with it, such as intermittency, process inflexibility, and poor energy efficiency. In the present work a 210 MW thermal power plant is integrated with LFR solar system with different thermal storage system. A MATLAB code is used as a simulation tool to analyse the performance of the solar integrated thermal cycle with two tanks and cascade thermal storage. The HTF plays a crucial role, and different HTFs have been considered in the present work. The impact of HTFs on the different parameters, such as outlet temperature of heat transfer fluids in the charging/discharging process, thermal efficiency of the storage system and total heat stored in the system during charging, has also been analysed. Stored energy is high in cascade TES, and that is 77.43 MW while with oil as HTF is 66.53 MW and two tank TES is 58.1 MW. The efficiency of TES with molten salt is 4.7% higher than oil. Improvement in performance parameters such as Fuel saving, Coal consumption rate, deemed saving of thermal energy and Efficiency with the cascade storage system is higher than two tank TES system.

Keywords: Linear Fresnel Reflector; Direct Normal Irradiance; Solar Integrated Thermal Cycle; Thermal Energy Storage; Phase Change Material; Heat Transfer Fluid, Cascade Thermal Storage.

1. Introduction

The use of renewable energy has been continuously increasing in the electricity generation because of the environmental issues associated with the conventional methods of power generation due to the use of fossil fuels. Sharma et al. (2020) discussed that among all alternative energy resources, solar energy is mostly used because of its abundance worldwide. Two methods are available to use solar energy, solar PV and CSP. Solar PV system works on the photovoltaic effect while in CSP technology heat transfer fluid is used to absorb the solar energy in the receiver. The concentrated solar power (CSP) technology has gained significant market share due to its high-capacity factor and economic competitiveness. Anchor et al. (2018) discussed that solar energy is available according to the time/ weather/ season and hence, it is not considered

* Corresponding author: Sharma Meeta
Amity University Uttar Pradesh, Noida (U.P.), India
Email: mitu0306@gmail.com

as a continuous source of energy. The discontinuity of solar energy can be avoided with the use of thermal storage with solar system. Sharma et al. (2020) stated the advantages of CSP solar system. CSP technology can be easily integrated with the TES and can produce continuous electricity. Garg et al. (2012) discussed the effect of thermal storage integration with the solar system. The stability of the power generation can be attained with the integration of an efficient TES system with CSP plant and thus it improves the plant efficiency. The CSP plant can deliver continuous dispatchable energy. Alva et al. (2017) discussed that the TES systems generally store heat in the two-form sensible heat and latent heat. Presently, most of the CSP plants in the world utilize two tanks as storage system. Pelay et al. (2017) explained about the two-tank sensible storage system. The HTF enters in the power cycle as well in the hot tank during charging process where it stores the energy. At the time of discharging the water absorbs the heat from the HTF in the hot tank. The cold tank is situated at the entry point of the solar field. The HTF received from hot tank is stored in cold tank for further use. The use of two tanks makes the system more costlier owing to the requirement of a larger volume for the storage tanks. Müller-Steinhagen et al. (2004) explained about the single-tank method, wherein the hot and cold materials are placed on the top and bottom, respectively. These are separated in a single tank due to their temperature difference. The thermocline effect can be enhanced with the addition of certain filler materials in the tank such as sand, quartzite rock, concrete etc. which can further decrease the quantity of storage material. The system with thermocline is less costly than two-tank storage by about 35% because of the savings in terms of the storage material, lesser storage volume being one storage. Nowadays latent heat storage systems are in use to enhance the performance of storage systems. Khandelwal et al. (2020) discussed that in comparison to sensible heat, the latent heat has a higher energy density, which leads to a lower requirement of volume for storage and thus a lower cost of the storage media. Cunha et al. (2016) elaborated methods to store and release the energy in latent heat energy storage. The HTF comes out from the receiver enters in the storage tank from the top. HTF transfers heat to PCM during the charging process then it starts to melt because its melting point is less as compared to HTF's temperature. Energy is stored during the charging process and this energy is absorbed by the HTF at the time of discharging process. Both sensible and latent heats are in trend for integration with CSP plants utilising two-tank and single-tank techniques.

PCMs play an important role in latent heat storage system to store the solar energy in daytime for further use. Beghi (2015) stated that the selection of appropriate PCM, surface of heat exchanger, and design of storage well-suited with the PCM are the three key components which effect the performance of the latent heat storage system. Prasad et.al. (2018) discussed the various desirable properties of PCM and techniques of using PCM in various thermal storage designs. With the use of PCM, the energy is stored as latent heat instead of sensible and a high quantum of energy at constant temperature is stored on account of the change of enthalpy during the change of phase of the storage material.

Khandelwal et al. (2022) discussed that the selection of the phase change material depends on the HTF in the solar receiver. HTF absorbs the heat in the solar receiver and transfers it for further use. The amount of absorbed energy depends on the nature of HTF. Pacio and Wetzel (2013) discussed different HTFs that can be used to absorb solar energy, such as water/steam, compressed air/gas, thermal oils, molten salt and liquid Na. Modi and Haglind (2014) explained that the use of water /steam as HTF makes the system more simplified and efficient because of no use of heat exchanger, and therefore electricity cost reduces. Rongrong et al. (2013) discussed that syntenic oil is also used as HTF, but its maximum temperature is limited to 400^0 C which restricts its use although it is an excellent heat transfer fluid. Above this temperature, it deteriorates very fast. In the present time, commercial CSP plants are mostly using organic oil, Therminol VP-1 as HTF.

Vignarooba et al. (2015) discussed that in the recent scenario, the range of temperature in the CSP plant is high in the range between

300-565^{0}C. So, for this high operating temperature range, molten salt is the most appropriate HTF as compared to oil and water. The molten salt can be used as HTF as well as a storage medium to collect the solar energy during the day. So, the selection of the HTF plays a very important role in CSP plant.

El Gharbi et al. (2011) and Peterseim et al. (2013) stated about the problem of standalone CSP plant. CSP plants are supplemented with a backup energy source during the periods of weaker solar intensity and in need of a faster response. There are many backup sources are available, like fossil fuels, natural gas, biomass, or solar photovoltaic. Natural gas has a commanding position as back up source of energy. Antonanzas et al. (2015) discussed about the hybridization of CSP system with a thermal power plant. It can provide uninterrupted power and can increase the plant efficiency. However, hybridization of CSP with the power cycle is new challenge to increase the market share due to the soaring prices of fossil fuels. The consistency, even with solar energy, can be realised by integration with TES system and/or with an appropriate hybridization option.

1.1. Problem Statement

The integration of a conventional system with a solar system is the most promising technology to minimize the problems associated with it. The CSP techniques have proven to be one with significant potential to generate electricity to meet the future energy demand without harming the environment. The main barrier behind its success is the variance of its availability with location and season, which results in intermittency. Integration of CSP plant with a conventional thermal plant with efficient TES, can avoid the associated intermittency. Generally, two ways are used to store the solar energy: two tanks and cascade TES. The best way to store solar energy is a latent heat storage system. Due to the integration of CSP with latent heat-based TES enhances the efficiency and effectiveness of the CSP system, leading to improved efficiency of the power plant. The designed TES system uses different type of PCM at different melting point temperatures. The PCMs have high latent heat and can change their phase from liquid to solid and solid to liquid at constant temperature by storing and releasing large amounts of energy and provide high energy storage capacity and target-oriented discharge temperatures.

In the present work a LFR system is used as a solar system and integrated with 210 MW thermal power plant. Two tank and Cascade TES has been integrated with the LFR solar system and analyzed the performance of thermal storage for different heat transfer fluids. According to the HTF appropriate PCM has been selected and analyzed the system. Our aim is to design a more efficient thermal storage system which can be integrate with Solar Integrated Thermal cycle to store the solar energy during the period of its non-availability.

This work demonstrates the real-time problem associated with the conventional thermal power plant. It also discusses the problem of the non-uniform availability of solar energy. The availability of solar energy is dependent on the time period and the weather. The work details the following aspects.

1. Integration of LFR as a CSP system with an already existing thermal power plant.
2. Design of Two Tank and Cascade TES by using different PCMs according to the used HTF, such as molten salt and oil.
3. Integration of the designed TES with SITC to provide continuous solar energy during its non-availability periods.
4. Analysis of the different parameters of Thermal Energy Storage with different HTFs during the charging and discharging process.
5. Comparison of the performance of the different Thermal Energy Storage for different HTF.
6. Comparison of the performance of Solar Integrated Thermal cycle for different TES.

The work discusses the optimal configuration of integration of a thermal storage system with a solar integrated thermal system, which provides the solution to real time problem associated with the thermal power cycle.

Nomenclature

T_{amb}	Ambient Temperature(^oC)
A	Solar Field Area (m^2)
Ar	Area of Receiver (m^2)
N_C	Number of Collectors
Aap	Net Aperture Area (m^2)
Q_i	Solar Collector Heat (kW)
(ΔT)	Thermal Storage Temperature Difference (K)
$C_{P,\ PCM}$	Phase Change Materials Specific Heat
m_{PCM}	Phase Change Material Mass (kg)
T_m	Mean Temperature (K)
R_{conv}	Covective Thermal Resistance ($^oC/W$)
$R_{subtank}$	Sub Tank Resistance ($^oC/W$)
$Q_{subtank}$	Subtank Heat Losses (kW)
$Q_{top\text{-}loss}$	Top Losses in Tank (kW)
$Q_{s,total}$	Stored Energy of Storage System (kW)
W_{net}	Network of Cycle (kW)
Q_B	Heat produced in Boiler boiler(kJ)
m_f	Fuel Mass Flow Rate (kg/s)
m_1, m_2--m_n	Mass flow Rate at Various State Condition in Thermal Cycle (kg/s)
W_{ISTT}	Turbine Work of Solar Integrated Thermal Cycle (kW)
W_{ISTP}	Pump Work of Solar Integrated Thermal Cycle (kW)
$T_{LFR,out}$	Outl Output Temperature at receiver (K)
$T_{ht,in}$	Hot Tank Input Temperature (K)
$T_{ht,0ut}$	Outlet Hot Tank Output Temperature (K)
Q_{htl}	Hot Tank Thermal Losses (kW)
Q_{ht}	Hot Tank Useful Heat (kW)
Q_{ctl}	Cold Tank Losses (kW)
Q_{hx}	Hot Salt Thermal Energy (kW)
Q_{ct}	Thermal energy of cold tank (kW)
$T_{ct,i}$	Cold Tank Input Temperature (K)
$T_{ct,o}$	Hot Tank Output Temperature (K)
U_{TES}	Global Heat Transfer Coefficient (W/m^2)
A_{TES}	Storage Tank Area (m^2)
σ	Stefan Boltzmann Constant
Q_{loss}	Receiver heat loss (W)
U_L	Coefficient of Heat Loss (W/m^2-K)
T_r	Receiver Temperature (^oC)
T_{sky}	Sky Temperature (^oC)
$(C_{p)\ htf}$	Heat Transfer Fluid's Specific Heat (kJ/kg-k)
$(\Delta T)_{htf}$	Heat Transfer Fluid's Temperature Difference (K)
U_{cond}	Conductivity (W/m^2-K)
L	Storage Tank Length (m)
m_{HTF}	Heat Transfer Fluid Flow Rate (kg/s)
R_{cyl}	Cylinder Thermal Resistance ($^oC/W$)
ρ_{HTF}	Heat Transfer Fluid Density (kg/m^3)
$Q_{total\text{-}loss}$	Total Thermal Losses (kW)
$Q_{hf,out}$	Heat Transfer Losses (kW)
Q_{LFR}	Heat of Solar Receiver (kW)
m_{mol}	Molten Salt Mass Flow Rate (kg/s)
$(C_{p)\ mol}$	Molten Salt Specific Heat (kJ/kg-K)
$(\Delta T)_{mol}$	Temperature Difference of Molten Salt(K)
$T_{out,m}$	Molten Salt Outlet temperature(K)
$T_{in,m}$	Molten Salt Inlet temperature (K)
$T_{LFR,in}$	Inlet temperature at receiver (K)
$T_{ht,min}$	Hot Tank Minimum Temperature (K)
$T_{s,i\ n}$	Input Temperature of Heat Transfer Fluid in Heat Exchanger (K)
$T_{s,out}$	Output Temperature of Heat Transfer Fluid at Heat Exchanger (K)
$T_{w,in}$	Inlet Temperature of Heat Transfer Fluid at Heat Exchanger (K)
$T_{w,out}$	Heat Exchanger Temperature (K)
M	Mass of molten salt (kg/s)
T	Circulation Time of Heat Transfer Fluid one cycle (hr)
V_{TES}	Thermal Storage Tank Volume (m^3)
ρ_{mol}	Molten Salt Density (kg/m^3)
W_T	Turbine work (kW)
W_p	Pump work (kW)
h_1,h_2,h_3,-----h_n	Enthalpy at Different State point cycle (kJ/kg)

Abbreviations

CSP	Concentrated Solar Power
CEP	Condensate Extraction Pumps
HTF	Heat Transfer Fluid
SHX	Solar Heat Exchanger
FWH#	Feed Water heater
SITC	Solar Integrated Thermal Cycle
HPT	High Pressure Turbine
TES	Thermal Energy Storage
PCM	Phase Change Material
LFR	Linear Fresnel Reflector
DNI	Direct Normal irradiance
IPT	Intermediate Pressure Turbine
LPT	Low Pressure Turbine
TP	Thermal Power

Subscripts

B	Boiler
C	Condenser
Sol	Solar
Ct	Cold tank
Co	Cover
D	Deaerator
FW	Feed Water Heater
Mol	Molten Salt
Ht	Hot Tank
Amb	Ambient
Ap	Aperture
H	Heat Transfer Fluid

2. System Description

The present LFR system consists of the base modules of 15.56 m width and 44.8 m length, which have 16 parallel lines of 8 slightly curved primary reflectors of glass mirrors. The receiver system consists of a vacuum absorber tube and a secondary reflector, which is installed along the focal line. The design parameters used for LFR system are shown in Table 1.

The LFR system is integrated with the 210 MW thermal power plant. With the integration of the solar power cycle with the thermal power cycle, the performance of the cycle gets improved. There are various configurations possible for such integration. Figure 1 represents one such configuration wherein the solar field is used parallel to the FWH#6 of the thermal cycle. In the proposed system, six feed water heaters have been used. At the point 4, 5, 6, 7 and 8, steam is extracted from the turbine and enters the feedwater heaters 5, 4, 3, 2 and 1, respectively. The steam comes out from the turbine at point 9 and enters the condenser. The feed water from the condenser enters the different feedwater heaters and absorbs the heat. The solar system has been integrated in parallel to the FWH# 6. The feed water at the exit of FWH# 5 leaves at point 21 and enters into SHX where it receives the heat from HTF. Then this feed water enters the boiler at point 24. FWH#6 can be replaced due to the integration of the solar system with the power cycle.

Table 1. Input parameters of LFR System Kurup et al. (2019)

Parameter	Value	Parameter	Value
Atmosphere temperature(°C)	20	Collectors Number	128
Location of latitude (°)	28.57	Net Aperture (m^2)	8,000
Longitude (°)	77.55	Concentration ratio	32
Wind Velocity (m/s)	5	Absorber's Inlet Diameter (m)	0.060
Solar Field Area (m^2)	32,000	Absorber 's Outer Diameter (m)	0.07
Average DNI (W/m^2)	550	Cover's Inside Diameter (m)	0.09
Optical Efficiency	0.93	Cover's Outer Diameter (m)	0.082
Collector Width (m)	15.56	Cover Emittance	0.88
Collector length (m)	44.8	Transmittance of Cover Plate	0.95
Inlet Temperature of HTF (°C)	200	Absorbance of Absorber	0.92
Outlet Temperature of HTF (°C)	257	Reflectance of Reflector	0.94

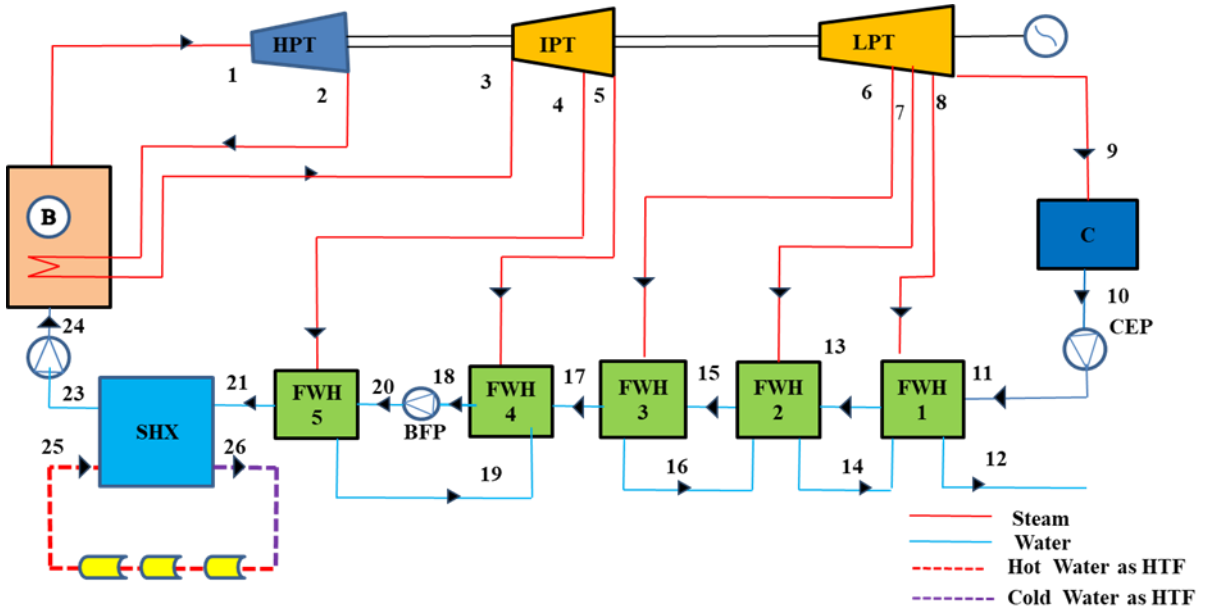

Fig. 1. Layout of Solar Integrated Thermal Cycle

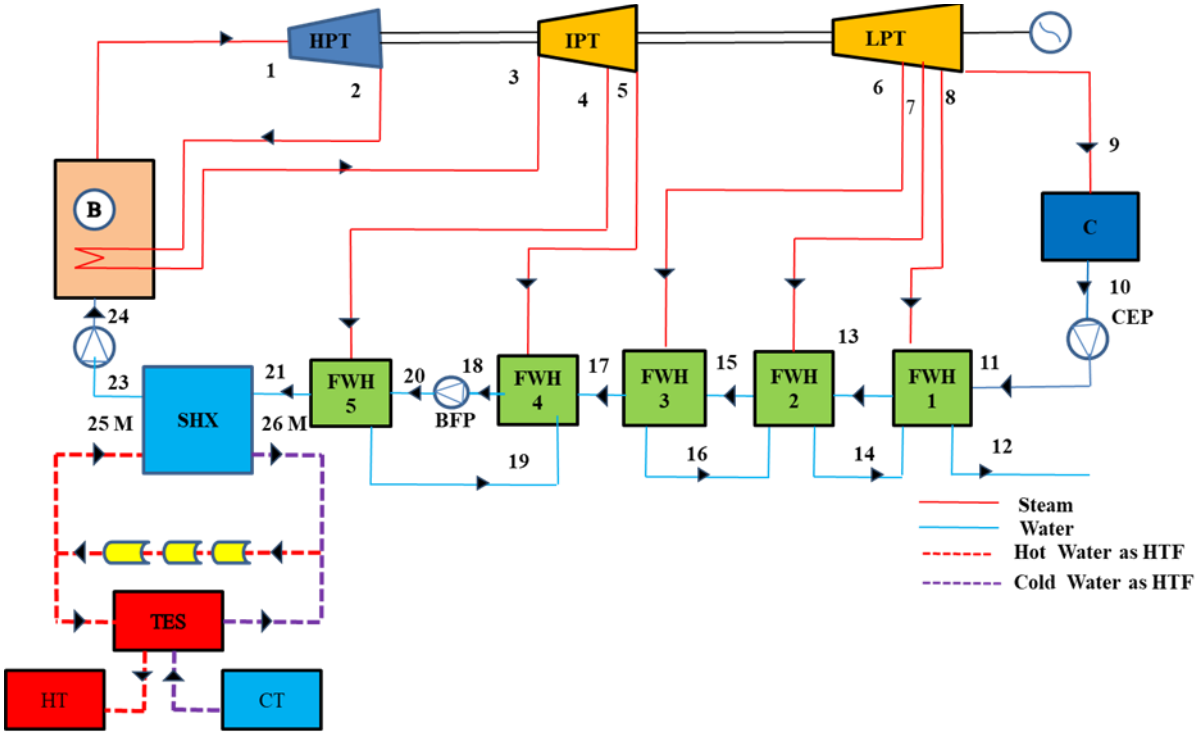

Fig. 2. Layout of Solar Integrated Thermal Cycle with Two Tank Thermal Energy Storage

Table 2. Properties of Molten Salt (Zhao et al. (2017))

Heat Transfer Fluid	Specific heat (kJ/kg-K)	Density (kg/m^3)	Operating Range of Temperature (°C)	Thermal Conductivity (W/m-K)
Molten salt	1.6	1870	265-564	0.52

Solar energy is absorbed in the absorber tube and carried by HTF for further use. In the present work, three HTFs such as water, Therminol oil, and molten salt are used. The different HTFs have different physical and thermal properties. The different properties of these HTFs have been shown in Table 2. Solar energy has been stored by thermal storage during the day for further use during its non-availability periods. Two types of storage systems have been considered in the present work, Two tank system and the cascade TES.

In the two-tank thermal storage system, molten salt is used as storage material as well as HTF. HTF absorbs the heat in the receiver then enters into the SHX and simultaneously in the hot tank. The hot molten salt discharges its heat to the water when solar energy is not available to increase its temperature for the conversion of steam. After transferring its heat to water, HTF enters the cold tank from where it is again reused in the receiver. Table 2 shows the different properties of Molten salt used as HTF in the present work.

In Fig. 2, it has been shown that with the integration of two tank system replacement of one feed water is possible. The feed water enters at state point 21 in SHX and comes out at 23. The HTF enters in the SHX at 25M, and the hot tank simultaneously and then return back in the cold tank at 26 M.

Figure 3 shows the layout of the Solar Integrated Thermal cycle with a cascade thermal storage system. The designed cascade storage system has a shell and tube heat exchanger, which consists of a carbon steel shell divided into three subsections vertically. According to Albanna et. al. (2017) the three PCMs ($NaNO_3$, $NaNO_2$, eutectic 40% KNO_3-60% $NaNO_3$) is selected for oil as HTF. The mixture of NaCl+52% $MgCl_2$(PCM1), mixture of Li_2CO_3+33% Na_2CO_3+ 35%K_2CO_3 (PCM2),

mixture of 59.98 wt% $MgCl_2$+20.42 wt% KCl+19.6 wt% NaCl (PCM3) and mixture NaCl/5.0% $NaNO_3$ (PCM4) is selected for molten salt as HTF. The inlet temperature of HTF is 395°C and 525°C for oil and molten salt respectively when enter in the TES during the charging process. The different sub-sections from the higher to lower melting temperature in the flow direction of the charging process. The shell contains carbon steel pipe submerged in the PCMs, where the HTF flows inside the tube.

In real CSP plants, the heat transfer fluid is heated up with the absorption of energy from the sunlight, which is concentrated in mirrors or lenses. When it is heated up, part of the HTF flows into the vertical storage tank from the top. During this process, HTF releases its energy by convection to the storage medium (i.e., phase change materials) while the other part enters into a heat exchanger to produce steam to drive a steam turbine coupled by a generator to generate electricity. The fluid coming from the CSP plant enters the tank at 27 M a specified temperature. As it moves downward, its temperature decreases (utilizing the concept of thermal stratification). On its way, HTF releases its energy to each PCM in the four containers as they keep heating until they reach their melting point temperatures and start to melt. When they are completely liquids they are fully charged and ready for discharging. On the other hand, in the discharging process, HTF coming back from the heat exchanger enters the storage tank at 29 M from the bottom with low temperature. As it moves upward in the tank, it gains heat from the lower melting temperature PCM to the higher at the top of the tank, acquiring all the possible energy from the PCMs as they solidify. Then, the heated HTF exits the storage tank at 30M with high temperature, which is used in the heat exchanger to generate steam and electricity.

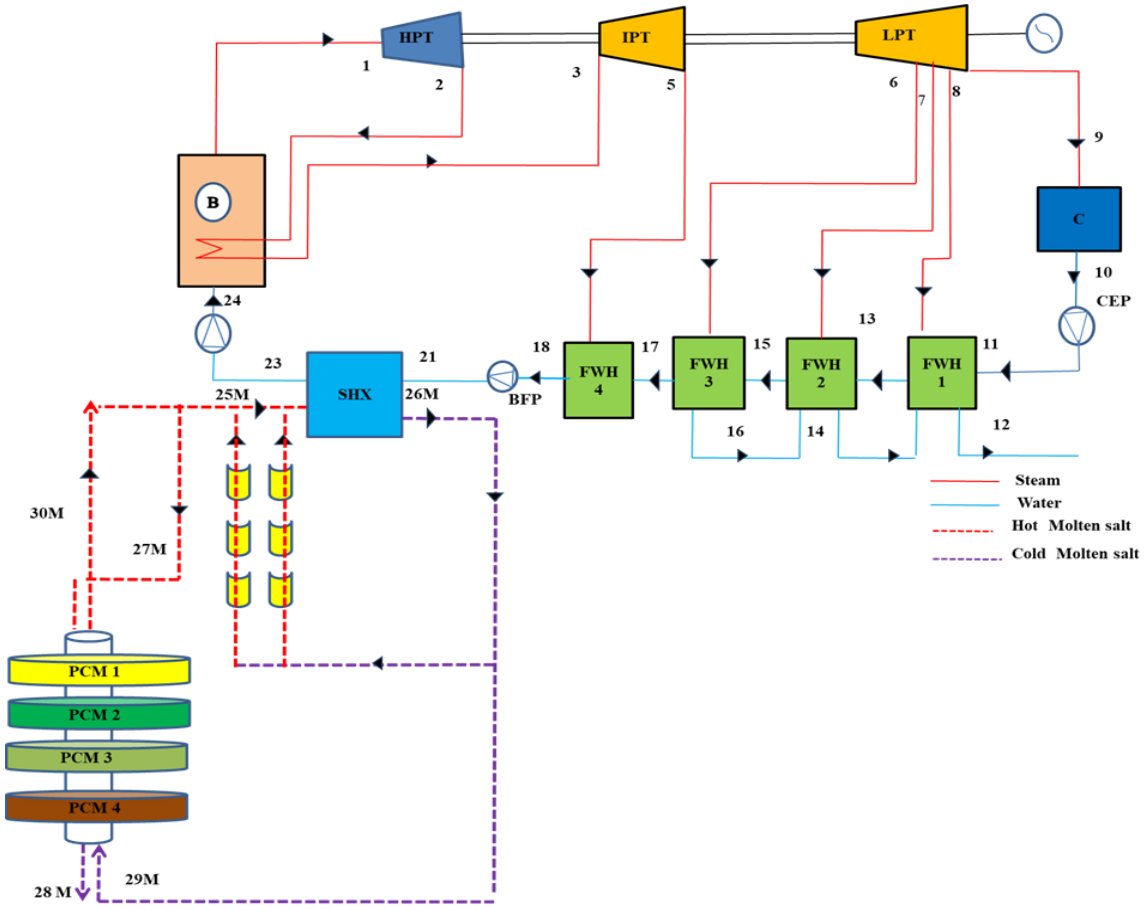

Fig. 3. Layout of Solar Integrated Thermal Cycle with Cascade Thermal Storage System

Table 3. Thermodynamic Properties at state points corresponding to Fig. 1, Fig. 2 and Fig. 3, Kumar et al. (2014,) and Vir (2012)

State Point	Working Substance	Pressure (bar)	Temperature (°C)	Specific enthalpy (kJ/kg)	Mass flow Rate (kg/s)
1	Water	150	538	34113.22	193.58
2	Water	40.60		3095.14	17.96
3	Water	36.62	538	3490.26	159.94
4	Water	15.88	425	3312.76	9.65
5	Water	8.57	310	3080.64	9.59
6	Water	2.27	196.1	2860.77	7.34
7	Water	0.852	106.90	2689.34	4.42
8	Water	0.413		2595.76	5.70
9	Water	0.1034		2415.12	122.54
10	Water	0.1034	46.21	193.50	12.87
11	Water	19.30	46.43	196.35	142.39
12	Water		76.34	319.52	17.60
13	Water		49.12	205.68	142.40
14	Water		95.12	398.12	12.01
15	Water		72.70	304.90	142.40
16	Water		125.90	519.34	7.32
17	Water		120.90	509.03	142.40
18	Water	8.42	160.80	678.59	193.58
19	Water		171	719.96	27.60
20	Water	205.65	164.20	789.09	177.50
21	Water		207	879.80	22.52
22	Water	200	200	859.99	177.50
23	Water	200	247	1071.97	177.50
24	Water	64.20	280	1233.30	177.50
25	Water	64.20	525.81	1039.50	110.80
26	Water	64.20	224	1015.90	177.50
25M	Molten Salt	64.20	525.81	1039.50	110.80
26 M	Molten Salt		300	745.98	110.80
27M	Molten Salt	64.20	525.81	1039.50	110.80
28M	Molten Salt	64.20	315	805.80	110.80
29M	Molten Salt	64.20	300	745.98	110.80
30M	Molten Salt	64.20	498.75	939.91	110.80

2. Flowchart

To analyse the performance of cascade thermal storage integrated with a solar system, a mathematical model was developed. This model has been analysed by developing MATLAB code. Figure 4 shows the flowchart that describes the methodology used to simulate this work.

3. Mathematical Modelling of SITC with Different Thermal Energy Storage

In the present work, the solar system is integrated with the cascade thermal storage system. The mathematical modelling has been carried out for the solar field as well as the cascade thermal storage system.

3.1. Solar Field

The LFR solar system located at 28.57°N, 77.55°E at an average elevation of 216m has been considered for the design and development of the thermodynamics model.

The heat absorbed by the collector is calculated as

$$Qi = Ar \times DNI \times Nc \tag{1}$$

According to Duffie et al. (2013), the different losses affected the energy received by the solar receiver. The energy received by the receiver is expressed as:

$$Qu = Aap \times \eta_{opt} \left[DNI - Q_{loss} \right] \tag{2}$$

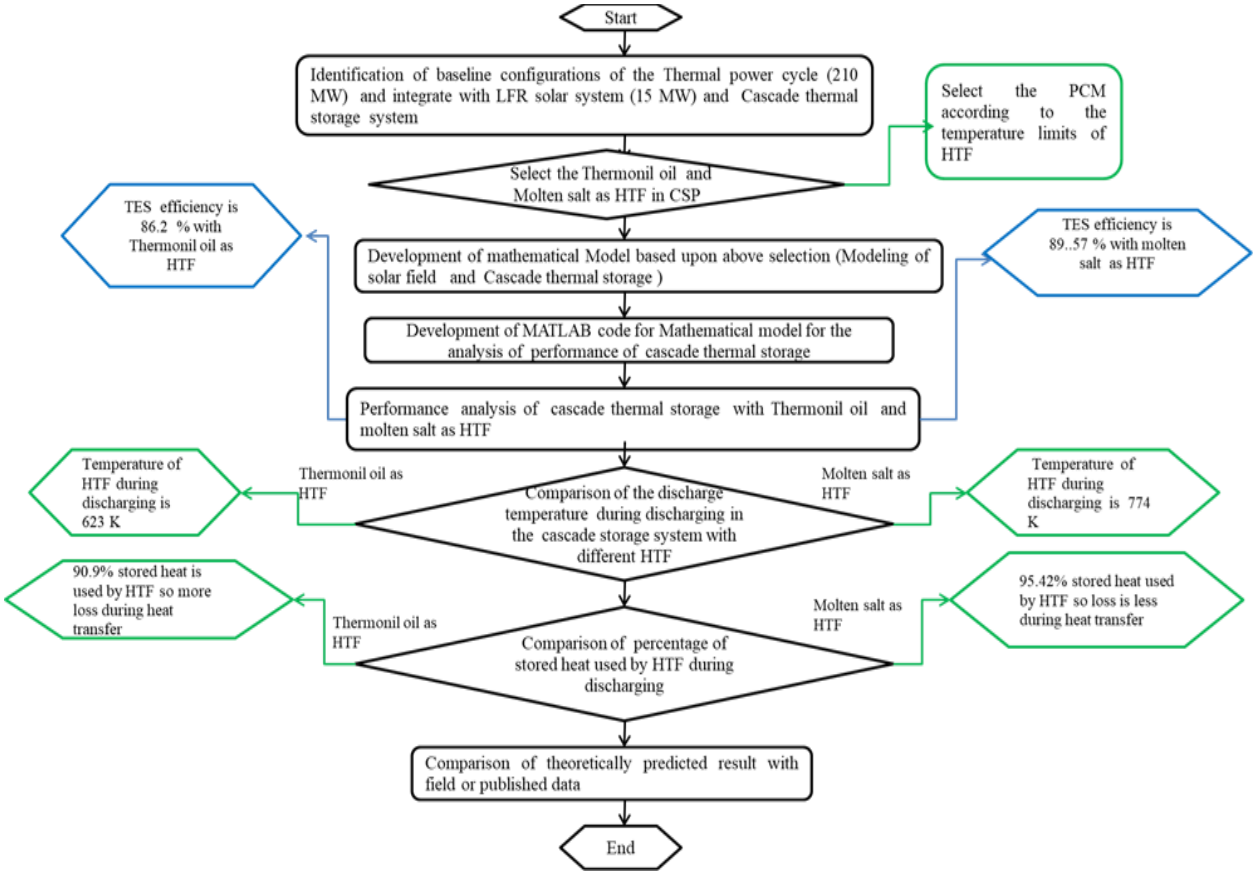

Fig. 4. Flowchart for the Simulation of Cascade Thermal Storage System

According to Duffie et al. (2013), from the surface, the heat transfer takes place due to convection and radiation, while from the support structure with conduction has been considered. The heat loss at the receiver is defined as

$$Q_{loss} = U_L \times (T_r - T_a)$$
$$U_L = (\mathrm{h}_w + h_r + U_{cond}) \times (T_r - T_a) \quad (3)$$

The optical efficiency of the collector is defined according to Mokheimer et al. (2014)

$$\eta_{opt} = \eta_o \times \mathrm{K}_{\mathrm{IAM}} \quad (4)$$

where the modifier of angle of incidence is 'K_{IAM}' and is defined as. Mokheimer et al. (2014).

$$K_{IAM} = K_{\perp}(\theta_{\perp}) \times K_i(\theta_i) \quad (5)$$

where $\mathrm{K}_{\perp}$ is the product-specific correction factor of transversal, K_i is product-specific correction of incident, $\theta_{\perp}$ is the Transversal angle and θ_i is the Incidence angle.

The temperature of HTF increases due to the heat absorption in the receiver. The heat absorbed by the HTF is further used in the power cycle, which is defined as Desai and Bandyopadhyay (2015)

$$Q_{solar} = \dot{m}_w \times C_{pw} \times (\Delta T) \quad (6)$$

3.2. Solar Integrated Thermal Cycle

The present study discusses a 210 MW thermal power plant that is integrated with LFR solar system. The solar system is integrated in parallel with FWH# used in the thermal cycle, which replaces the feedwater heater from the cycle. Thermal efficiency of the power cycle improves because of the replacement of FWH#. The turbine work and pump work of the power cycle is defined as

$$W_T = \dot{m}_{in} \times \left(h_{in} - h_1\right) + \sum_{n=1}^{n=m} (\dot{m}_{in} - \dot{m}_n - \dot{m}_{n-1} - \dot{m}_{n-m}) \times \left(h_{T,\mathrm{out}} - h_{T,\mathrm{in}}\right) \quad (7)$$

$$W_P = \sum_{n=1}^{n=m} (\dot{m}_{in} - \dot{m}_n - \dot{m}_{n-1} - \dot{m}_{n-m}) \left(h_{P,\text{out}} - h_{P,in}\right) + \dot{m}_{in} \times \left(h_{20} - h_{18}\right) \quad (8)$$

Net work of the cycle is defined as

$$W_{net} = \Sigma W_T - \Sigma W_p \quad (9)$$

Heat supplied in the boiler and the efficiency of the cycle is defined as

$$\dot{Q}_B = \dot{m}_{in} \times \left(h_1 - h_{23}\right) + (\dot{m}_{in} - \dot{m}_1) \times \left(h_3 - h_2\right) \quad (10)$$

$$\eta_{th} = \frac{w_{net}}{\dot{m}_f \times C.V} \quad (11)$$

As discussed, the replacement of feed water is dependent upon the available solar energy. The replacement of FWH# reduces the steam extraction from the steam turbine, and that is defined as

$$\dot{m}_1 = 0, \dot{m}_2 = 0 - - - - - - \dot{m}_n = 0$$

So the turbine work of ISTC is defined as Ahmadi et al. (2019)

$$W_{ISTT} = \dot{m}_{in} \times \left(h_{in} - h_1\right) + \sum_{n=1}^{n=m} (\dot{m}_{in} - \dot{m}_n - \dot{m}_{n-1} - \dot{m}_{n-m}) \times \left(h_{T,out} - h_{T,\text{in}}\right) \quad (12)$$

The pump power is defined as Ahmadi et al. (2019)

$$W_{ISTP} = \sum_{n=1}^{n=m} (\dot{m}_{in} - \dot{m}_n - \dot{m}_{n-1} - \dot{m}_{n-m}) \times \left(h_{P,\text{out}} - h_{P,in}\right) + m_{in}) \times \left(h_{20} - h_{18}\right) \quad (13)$$

Network output of the power cycle is calculated after substituting the value of m_1, m_2, according to the available solar energy. Ahmadi et al .(2019)

$$W_{net} = \Sigma W_{ISTT} - \Sigma W_{ISTP} \quad (14)$$

The thermal efficiency of the Solar Integrated Thermal cycle is defined as Achour et al., 2018.

$$\eta_{th} = \frac{W_{net}}{\dot{m}_f \times CV + Q_{solar}} \quad (15)$$

3.3. Two Tank Thermal Energy Storage

Solar receiver used molten salt as HTF, which is also used to store solar energy in a storage tank. Heat received by the collector system is defined according to Achour et al. (2018).

$$\dot{Q}_{LFR} = DNI \times A_{ap} \times \eta_{opt} \quad (16)$$

HTF (molten salt) flows in the receiver and absorbs the heat. It is defined as (Zhao et al. (2017)

$$\dot{Q}_{LFR} = \dot{m}_{mol} \times (C_p)_{mol} \times (\Delta T)_{mol} \quad (17)$$

Each HTF has its operating temperature limits. For this fixed value, calculate the maximum mass flow rate in the solar receiver. That is calculated according to Zhao et al. (2017),

$$\dot{m}_{mol} = \frac{\dot{Q}_{LFR}}{(C_p)_{mol} \times (\Delta T)_{mol}} \quad (18)$$

For the calculated mass flow rate and useful solar heat, the actual temperature at the exit of the receiver is defined as Zhao et al. (2017).

$$\dot{Q}_U = \dot{m}_{mol} \times (C_p)_{mol} \times \left(T_{LFR,\text{out}} - T_{LFR,in}\right) \quad (19)$$

$$T_{LFR,\text{out}} = \frac{\dot{Q}_u}{(C_p)_{mol} \times \dot{m}_{mol}} + T_{LFR,in} \quad (20)$$

3.3.1. Hot Tank Model

In the two-tank model, two tanks i.e., hot and cold tank are used. The HTF coming out from the receiver enters the power cycle. Simultaneously, some amount is entered in the hot tank to store the energy for further use when it's not available. $T_{LFR,o}$ is the output temperature of the receiver while Th,i is the temperature at the input of hot tank. Various losses take place during heat transfer in the tank, which affects the performance of the storage system. According to Zhao et al. (2017)

$$T_{LFR,0} = T_{ht,i} \quad (21)$$

$$\dot{Q}_{htl} = U_{TES} \times A_{TES} \times \left(T_{ht,i} - T_a\right) \quad (22)$$

where, U_{TES} is considered as the coefficient of global heat transfer t and T_a is the atmospheric temperature [27]

Total mass of HTF (molten salt) is calculated according to Zhao et al. (2017) is,

$$M = \dot{m}_{mol} \times T = V_{TES} \times \rho_{mol} \quad (23)$$

where storage time is T, and it is assumed to be two hours [21] in the present analysis. By considering the losses temperature at the exit of the hot tank is calculated as Zhao et al.(2017)

$$\dot{Q}_{ht} = \dot{Q}_u - \dot{Q}_{htl} = \dot{m}_{mol} \times (C_p)_{mol} \times \left(T_{ht,i} - T_{ht,o}\right) \quad (24)$$

$$T_{ht,out} = T_{ht,i} - \frac{\dot{Q}_{ht}}{\dot{m}_{mol} \times (C_p)_{mol}} \quad (25)$$

3.3.2. Load Model

In the storage tank, molten salt should be in liquid state. So, the temperature of the HTF should control to avoid freezing. So, the stop temperature has been considered to control the heating temperature. Zhao et al. (2017),

$$T_{stop} = \frac{\dot{Q}_l}{(C_p)_{mol} \times \dot{m}_{mol}} + T_{ht,\min} \quad (26)$$

The heat is transferred between salt and water during the discharging process. So, the temperature of the salt is calculated as

$$T_{s,out} = T_{s,\text{in}} - \frac{T_{\text{w,out}} - T_{\text{w,in}}}{\in_{hx}} \quad (27)$$

3.3.3. Cold Tank Model

After transferring the heat the HTF enter in the cold tank and is stored there for further use. The temperature at the input of the cold tank is defined as Zhao et al. (2017)

$$T_{s,out} = T_{ct,\text{in}} \quad (28)$$

The thermal losses in the cold tank are calculated as.

$$\dot{Q}_{ctl} = U \times A \times \left(T_{ct,in} - T_a\right) \quad (29)$$

In a heat exchanger, the energy is transferred by the salt to water. it is defined as

$$\dot{Q}_{hx} = (C_p)_{mol} \times \dot{m}_{mol} \times \left(T_{ht,\text{out}} - T_{s,out}\right) \quad (30)$$

Stored energy in the cold tank is calculated as

$$\dot{Q}_{ct} = \dot{Q}_{hx} - \dot{Q}_{ctl} = (C_p)_{mol} \times \dot{m}_{mol} \times \left(T_{ct,\text{in}} - T_{ct,\text{out}}\right) \quad (31)$$

The temperature at the exit of the cold tank is defined as

$$T_{ct,\text{out}} = T_{ct,\text{in}} - \frac{\dot{Q}_{ct}}{(C_p)_{mol} \times \dot{m}_{mol}} \quad (32)$$

3.4. Cascade Thermal Energy Storage

The proposed cascade thermal storage system is designed for different HTFs. According to the HTFs, different layers of PCM have been used because the PCMs used in thermal storage are dependent on the temperature limits of HTFs used. In the present work, molten salt and therminol oil are considered as HTFs. Table 4 shows different properties of PCMs used according to the nature of HTFs.

3.4.1. Design Parameters used for Storage System

According to HTFs, the PCM for the storage system is selected. In the present work, two types of HTFs for a cascade storage system are analysed. Table 5 and 6 show the properties of different PCM's according to the Therminol oil and Molten salt.

Table 4. The properties of HTF oil and molten salt. (Albanna et al.2017) and (Wei et al. 2018)

Storage medium	Water	Thermal oils	Molten Salt
		Silicone oil (Biphenyl /Diphenyl oxide)	Nitrate Salt
Melting Point Temperature. (^{o}C)	0	12	265
Stability limit (^{o}C)	100	400	565
Density (kg/m^{3})	1000	900	1870
Thermal conductivity (W/m- K)	0.598	0.10	0.52
Heat capacity (kJ/kg- K)	4.18	2.1	1.6

Table 5. Properties of PCM used with oil as HTF. Albanna et al. (2017)

Description	PCM1 ($NaNO_3$)	PCM2 ($NaNO_2$)	PCM3 (40% KNO_3 +60% $NaNO_3$)
Melting point temperature (°C)	308	271	220
Solidification temperature	308	271	220
Latent heat (kJ/kg- K)	200	195	108.76
Density (kg/m^3)	2257	2168	1725
Thermal conductivity (W/m-K)	1	1	0.5
Solid specific heat capacity (kJ/kg-K)	1.8227	1.6	1.52

Table 6. Properties of PCM used for HTF (Molten Salt) used in solar receiver. Wei et al. (2018)

Description	PCM1 NaCl+52% $MgCl_2$	PCM2 Li_2CO_3+ 33%Na_2CO_3 +35%K_2CO_3	PCM3 $MgCl_2$+ 20.42%KCl +19.6 % NaCl	PCM4 NaCl+5.0%$NaNO_3$
Melting point temperature (°C)	450	397	347	284
Solidification temperature	450	397	347	284
Latent heat (kJ/kg K)	431	277	198.3	171
Density (kg/m^3)	2225	2200	2118	2000
Thermal conductivity (W/m-K)	2	1	1	0.5
Specific heat capacity (kJ/kg K)	1.33	1.03	.928	1.21

Table 7. Performance parameters used to design cascade TES Elfeky et al. (2020)

Parameters	Design Value
Mass of phase change material (m_{PCM})	$3.066*10^5$ kg
Height of the tank (H) (Molten salt)	6.62 m
Diameter of the Tank (D_{tank}) (Molten salt)	10.5m
Heat transfer coefficient of HTF for convection	5.038 (W/m^2-K)
Required power for frictional losses (W_p)	1.14 MW
Heat transfer coefficient of the air (h_{air})	8.34 (W/m^2-K)
Radius of pipe (m)	0.3012 (m)
Friction coefficient (f)	0.0126
Thermal conductivity of insulation (K_{in})	0.06 (W/m-K)
Thermal conductivity of air (K_{air})	0.03525 (W/m-K)
Velocity of air (v_{air})	$3.188*10^{-5}$(m/s)
Thermal diffusivity ($\tilde{\alpha}$)	$4.55*10^{-5}$ (m^2/s)
Roughness of carbon steel is ε	0.05 mm

Cascade TES has different design parameters for different HTF is distinct. The different parameters used to design storage system is shown in Table 6.

To design the storage system, the initial storage capacity is assumed as the two-tank TES, which is designed for 8 hours. The energy of the storage system is defined as

$$Q_{TES} = m_{PCM} \times C_{p,\mathrm{PCM}} \times \Delta T \tag{33}$$

The designed cascade storage system has different sub tank with different PCM(s). Each PCM has different melting point temperature and specific heat. The total capacity of the storage system is defined as Albanna et al. (2017).

$$Q_{TES} = m \times [(C_{p,pcm1} \times \Delta T_1) + (C_{p,pcm2} \times \Delta T_2) + (C_{p,pcm3} \times \Delta T_3) + (C_{p,pcm4} \times \Delta T_4)$$
$$m_{PCM2} = m_{PCM2} = m_{PCM3} = m \tag{34}$$

So, the stored energy in the storage system is,

$$Q_{TES} = m\times[(C_{p,pcm1}\times\Delta T_1)+(C_{p,pcm2}\times\Delta T_2)+(C_{p,pcm3}\times\Delta T_3)+(C_{p,pcm4}\times\Delta T_4) \quad (35)$$

Required PCM mass is estimated as Albanna et al. (2017)

$$m_{pcm} = \frac{Q_{TES}}{[(C_{p,pcm1}\times\Delta T_1)+(C_{p,pcm2}\times\Delta T_2)+(C_{p,pcm3}\times\Delta T_3)+(C_{p,pcm4}\times\Delta T_4)} \quad (36)$$

Different PCMs have different densities, so they occupy different volumes. So, the height of each sub tank is different. The height of the sub tank is defined for the given mass according to Albanna et al. (2017)

$$m_{PCM} = \rho_{PCM}\times V_{PCM} = \rho_{PCM}\times\Pi\times\left(\frac{D^2_{tank}-D^2_{pipe}}{4}\right)\times H \quad (37)$$

$$H = \frac{m_{PCM}\times 4}{\rho_{PCM}\times\Pi\times\left(\frac{D^2_{tank}-D^2_{pipe}}{4}\right)} \quad (38)$$

The total height of the storage tank is estimated as

H=H1+H2+H3+H4

where height of the subtank1, subtank2 and subtank3 are H1, H2 and H3, respectively.

3.4.2. Thermal Storage Capacity and Efficiency Calculation

It is not possible that the energy available with the HTF is completely stored in the TES due to the various losses which is associated with the flow of HTF in TES. So, the storage energy is calculated considering these losses. According to the energy conservation law, the stored energy is defined as Albanna et al. (2017)

$$Q_{in} = Q_{stored}+Q_{loss}+Q_{htf,out} \quad (39)$$

$$Q_{stored} = Q_{in}-Q_{loss}-Q_{htf,out} \quad (40)$$

where Q_{loss} is the total loss that takes place in the storage tank, which considers different type of losses of sub tank. Each sub tank consist different PCM so it possesses different properties. The losses for each tank have been calculated separately. According to (Tay et al. 2012), the Fig. 5 shows the thermal resistance which is defined as.

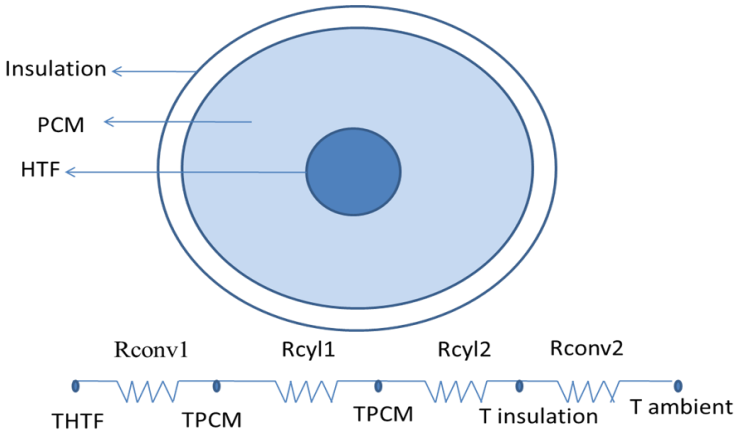

Fig. 5. Radial -axis thermal resistance

$$R_{sub\ tank} = R_{conv.1}+R_{cyl,1}+R_{cyl,2}+R_{conv,2}$$

$$= \frac{1}{h_{HTF}\times A_{s,pipe}}+\frac{\ln(r_{tank}/r_{pipe})}{2\Pi\times H_{sub\ tank}\times K_{PCM}}+\frac{\ln(r_{tank}/r_{pipe})}{2\Pi\times H_{sub\ tank}\times K_{PCM}}+\frac{1}{h_{air}\times A_{s,tank}} \quad (41)$$

$$Q_{sub\,\text{tank}} = \frac{T_{HTF} - T_A}{R_{sub\,\text{tank}}} \quad (42)$$

where T_A is the atmosphere temperature. According to Khandelwal et al. (2022), the total loss is defined as:

$$Q_{total-loss} = Q_{sub\,\text{tank}\,1} + Q_{sub\,\text{tank}\,2} + Q_{sub\,\text{tank}\,3} \quad (43)$$

$$R_{top} = R_1 + R_2 + R_{conv}$$

$$\frac{L_{\text{subtank}\,1}}{K_{PCM1} \times A_{\text{c,tank}}} + \frac{L_{insulation}}{K_{insulation} \times A_{\text{c,tank}}} + \frac{1}{h_{air} \times A_{\text{c,tank}}} \quad (44)$$

$$Q_{top-loss} = \frac{T_{PCM1} - T_A}{R_{top}} \quad (45)$$

where R_{top} is the top tank resistance (^{o}C/W) .

The efficiency of TES is defined as

$$\eta_{TES} = \frac{Q_{stored}}{Q_{in}} \quad (46)$$

where Q_{in} is the total heat transferred by the HTF in thermal storage.

4. Results and Discussion

The thermodynamic model is developed to simulate the solar cycle and evaluate the impact of its integration with a conventional thermal power cycle on various performance parameters using different heat transfer fluids (HTFs) and thermal energy storage (TES) systems. The amount of solar energy available for utilization depends on the type of HTF and the solar irradiation. The selected HTF also influences the performance of the thermal storage system. The performance of different TES configurations and their integration with the integrated solar thermal cycle (ISTC) has been modelled using MATLAB, and the results have been presented and analysed.

4.1. Variation of Temperature Difference for Different HTF's

As discussed, at the charging process, the HTF enters in the TES with a higher temperature than the melting point of PCM. The temperature difference exist in TES is affected by the type of HTF used in the receiver. In the present work, two HTFs (oil and molten salt) have been used in a solar receiver. Figure 6 shows the variation of temperature in TES with DNI for different seasons with oil as HTF. The temperature difference is 219.60^{o}C, 212.98^{o}C, 207.19^{o}C and 172.34^{o}C in summer, autumn, spring, and winter, respectively. The temperature difference with Therminol oil is almost similar to that of Albanna et.al. (2017) which is 195^{o}C.

Figure 6 shows the variation of temperature difference in the TES using oil as the HTF for different seasons. The achievable outlet temperature of the HTF from the receiver is higher when molten salt is used instead of oil, owing to its higher operating temperature range. Consequently, the inlet temperature of molten salt in the TES during the charging process is also higher. Figure 7 illustrates the variation of temperature difference in the TES with molten salt as the HTF for different seasons. The observed temperature differences are 311.74°C, 302.93°C, 295.23°C, and 248.87°C, respectively. Overall, the temperature difference is greater with molten salt as the HTF across all seasons.

4.2. Comparison of Temperature Variation Across Different Thermal Energy Storage Systems

Different heat transfer fluids (HTFs) exhibit distinct thermophysical properties and operating temperature limits, which directly influence the outlet temperature of the solar receiver. The inlet and outlet temperatures of the HTF in the thermal energy storage (TES) system determine the temperature gradient during the charging process, thereby affecting the overall heat storage capacity and efficiency. In the present study, the thermodynamic performance of two TES configurations—two-tank and cascade systems—has been analyzed. The comparative variation of temperature difference during the charging process for these TES systems is illustrated in Fig. 7.

The cascade TES system using molten salt exhibits a higher temperature difference compared to other configurations, while the two-tank storage system shows the lowest temperature difference. A higher temperature difference indicates a greater amount of heat stored in the TES during the charging process, which can be utilized for subsequent energy requirements.

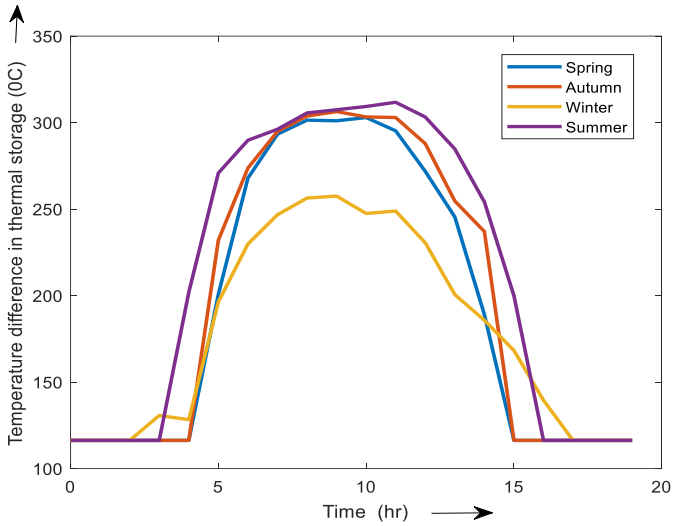

Fig. 6. Temperature Difference with Molten Salt HTF Across Seasons.

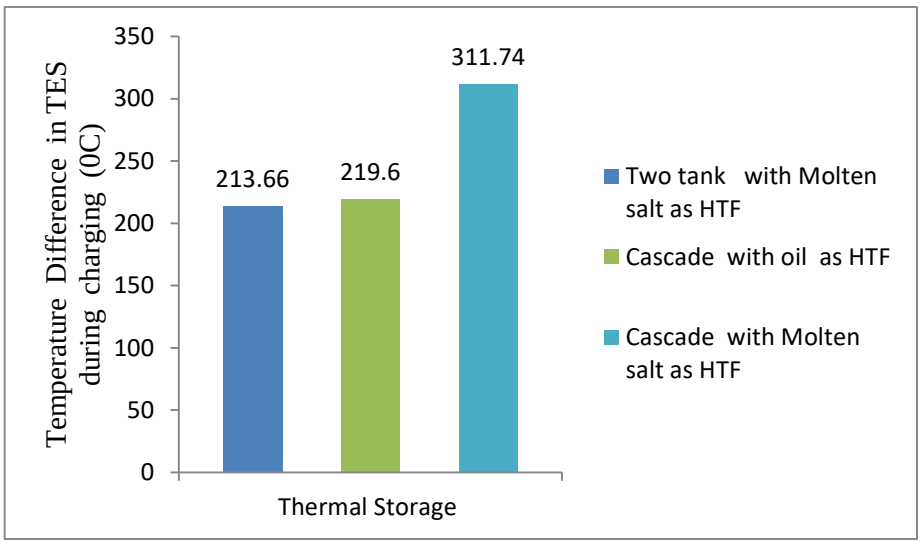

Fig. 7. Comparison of Temperature Difference Exist in Different TES

4.3. Comparison of Stored Heat During Charging Process

It is well known that the main limitation of solar energy is its unavailability during nighttime. The integration of a latent thermal energy storage (TES) system with the solar system enables the utilization of stored thermal energy during non-solar hours. In a two-tank system, the heat transfer fluid (HTF) enters the hot tank and stores energy in the form of sensible heat, which is later released to the working fluid when solar energy is unavailable.

In contrast, in a cascade TES system, the HTF enters the storage unit at a temperature higher than the melting point of the phase change material (PCM). During the charging process, the HTF transfers its heat to the PCM, causing it to melt and thereby store energy in the form of latent heat—a higher inlet temperature of the HTF during charging results in greater energy storage capacity. Figure 8 presents a comparison of the energy stored in different TES configurations using various HTFs. As discussed earlier, the cascade TES with molten salt as the HTF exhibits the highest temperature difference among all systems. Consequently, it also stores the maximum amount of energy—77.43 MW—compared to 66.53 MW for the cascade TES with oil and 58.1 MW for the two-tank TES system.

4.4. Comparison of Different TES Efficiency

The effectiveness of integrating a thermal energy storage (TES) system with a solar power system largely depends on the efficiency of the TES. A more efficient TES allows a greater amount of solar energy to be stored for later use. The efficiency is influenced by the temperature difference that exists within the TES during the charging process. As discussed earlier, the temperature difference is higher in the cascade TES using molten salt as the heat transfer fluid (HTF) compared to oil-based systems and the two-tank storage configuration. Due to this larger temperature difference, the cascade TES with molten salt is capable of storing more energy, thereby enhancing the overall storage efficiency.

Figure 9 illustrates the comparison of TES efficiencies for different HTFs. The maximum efficiency of 89.57% is achieved with the cascade TES using molten salt as the HTF, followed by 86.2% for the cascade TES with oil. The two-tank storage system exhibits the lowest efficiency among the analyzed systems, primarily due to higher thermal losses.

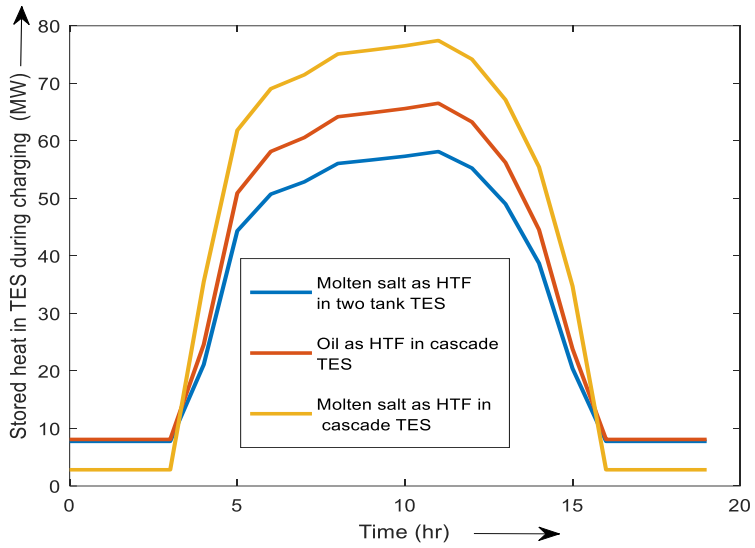

Fig. 8. Comparison of Stored Energy with Different HTF and TES

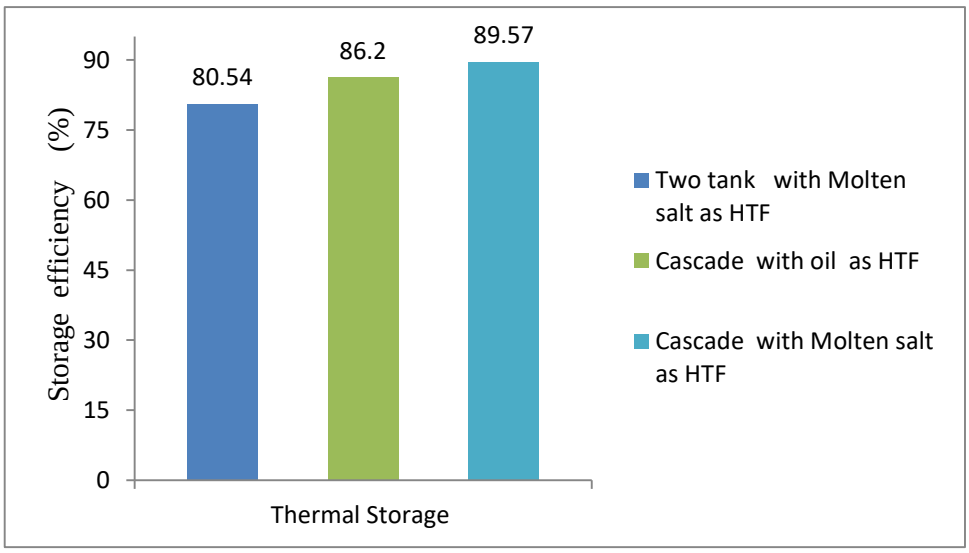

Fig. 9. Comparison of Thermal Storage Efficiency for Different HTFs

4.5. Comparison of Discharging Temperature for Different HTFs

Solar energy is stored in a storage system during charging due to the melting of the PCM used in it. This stored energy is discharged during times of solar energy unavailability. While HTF passes through the storage system during the discharging period, PCM starts to solidify and gives its heat to HTF increasing the temperature of HTF. The discharging temperature plays a vital role in the further use of this HTF for any applications, because the higher the discharging temperature, the more heat is available for further use. Figure 10 presents a comparison of the discharging temperatures for different TES configurations and HTFs. In the cascade system, the discharging temperatures are 350°C with Therminol oil and 501°C with molten salt, while in the two-tank storage system, the discharging temperature is 476.25°C. The outlet temperature obtained using Therminol oil is consistent with the findings of Albanna *et al.* (2017), who reported a value of approximately 364°C.

4.6. Comparison of the Percentage of Stored Energy Use During Discharging Process for Different HTFs

The HTF, at a temperature above the PCM's fusion point, enters the TES, initiating melting of the PCM and the storage of thermal energy during charging. This stored energy is used by HTF during the discharging process and increases its temperature. It is not possible that when HTF passes through TES during the discharging process can absorb the complete stored energy, as some losses take place during heat transfer from PCM to HTF. Figure 11 shows the comparison of the percentage of stored energy used with different HTF during discharging, which affects the HTF's temperature during discharging. The amount of stored energy used by oil is 90.09% and 95.42% molten salt. The amount of stored heat collected by oil is in tune to Albanna et al. (2017)

4.7. Comparison of Different Parameters of SITC for Different Thermal Storage

The integration of the solar system enhances the efficiency of the thermal power cycle. In the present study, different types of thermal energy storage (TES) systems are considered for integration with the solar system to store energy during periods of solar unavailability. The solar system is coupled with an existing coal-fired thermal power plant, and the integration of TES with the integrated solar thermal cycle (ISTC) leads to improvements in various performance parameters.

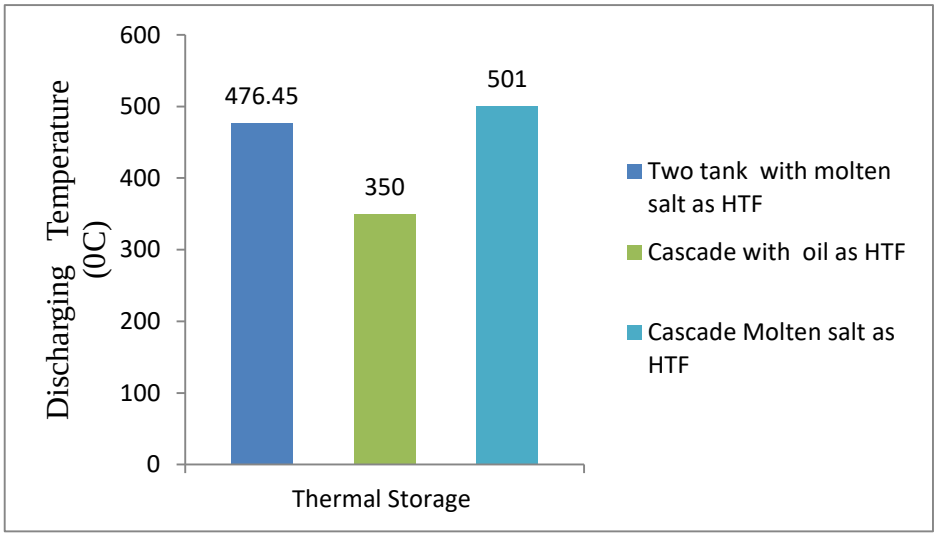

Fig. 10. Comparison of Discharging Temperature of Different HTFs

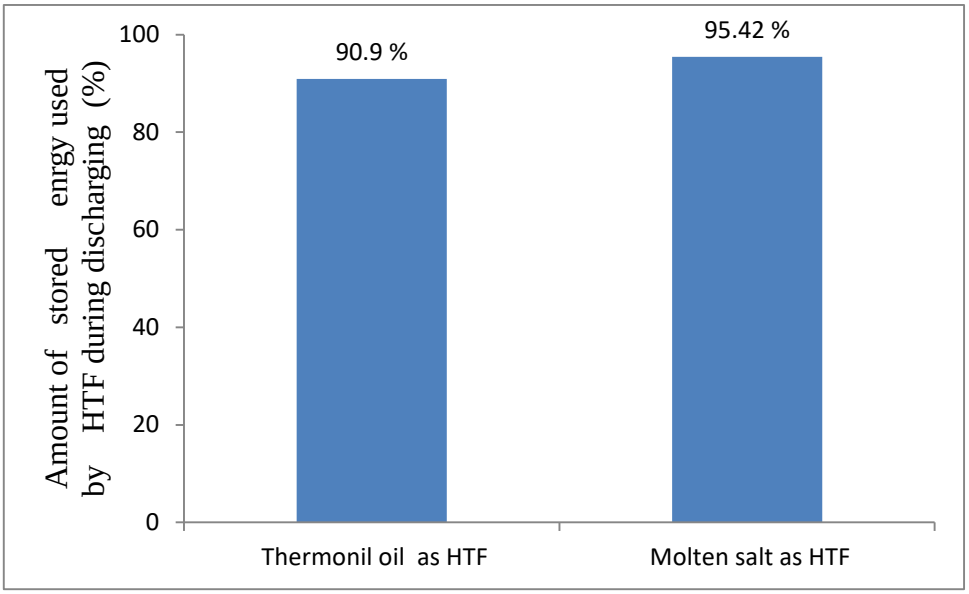

Fig. 11. Comparison of Percentage of Stored Energy Use During Discharging Process

4.7.1. Replacement of Feed Water Heater

In the present study, the solar system is integrated in parallel with the feedwater heaters (FWHs) of the conventional thermal power cycle, allowing partial or full replacement of the existing FWHs. Since solar energy is available only during the daytime, a thermal energy storage (TES) system is incorporated with the integrated solar thermal cycle (ISTC) to utilize the stored energy during periods of solar unavailability. In the ISTC system, the extent of FWH replacement depends on the amount of energy stored in the TES during the charging process. Two types of TES are considered in this study, and the quantity of stored energy differs between them, influencing the possible replacement of FWHs from the conventional cycle. Table 8 presents a comparison of the thermal energy stored in the different TES configurations and the corresponding FWH replacement potential.

4.7.2. Comparison of Saving of Thermal Energy SITC with Different TES.

With the integration of TES with the solar system, solar energy is stored during the day for further use. As discussed in the previous section, different amounts of energy can be stored with different types of TES which affect the replacement of FWH(s) from the cycle. This replacement of FWH(s) from the cycle affects the extraction of steam from the different state points of the turbine, which increases the turbine work. Corresponding to this increase in turbine work, the deemed saving of thermal energy is calculated in the present work. Figure 12 shows the comparison of the deemed savings of thermal energy for different TES.

Table 8. Comparison of Replacement of FWH(s) with Different Type of TES.

TES	Thermal Energy Stored (MW)	Replacement option	Discharging Time
Two Tank	58.1	FWH#6	2 hrs
Cascade TES oil as HTF	66.53	FWH#6	6 hrs
Cascade TES molten salt as HTF	77.43	FWH#5+6	6 hrs

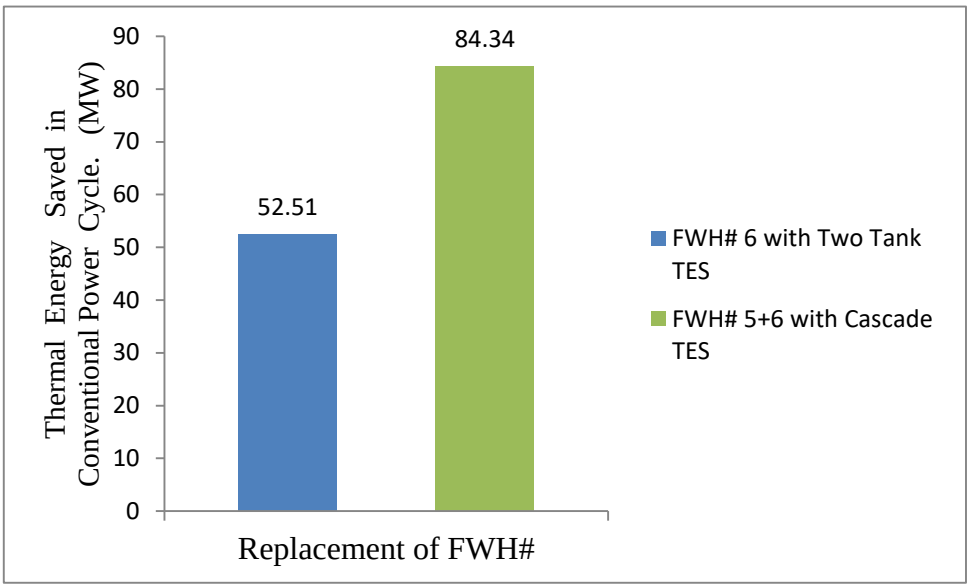

Fig. 12. Comparison of Deemed Saving of Thermal Energy of Different TES.

4.7.3. Comparison of SITC Thermal Efficiency with Different TES

Due to the replacement of FWH(s) from SITC cycle with the integration of TES, the net turbine output of the system improves, which increases the efficiency of the thermal power cycle. Improvement of the thermal efficiency depends on the number of FWH replacements. Replacement of FWH# 6 is possible with two-tank TES, while replacement of FWH# 5 and 6 with cascade TES with molten salt as HTF is possible because of the availability of more stored heat in cascade TES. Due to the two-feed water heater replacement with cascade TES, thermal efficiency improvement is more as compared to two tank TES. The enhancement in cycle efficiency due to integration is in agreement with Amano and Abbas (2017), where an improvement of 1.04% was noted.

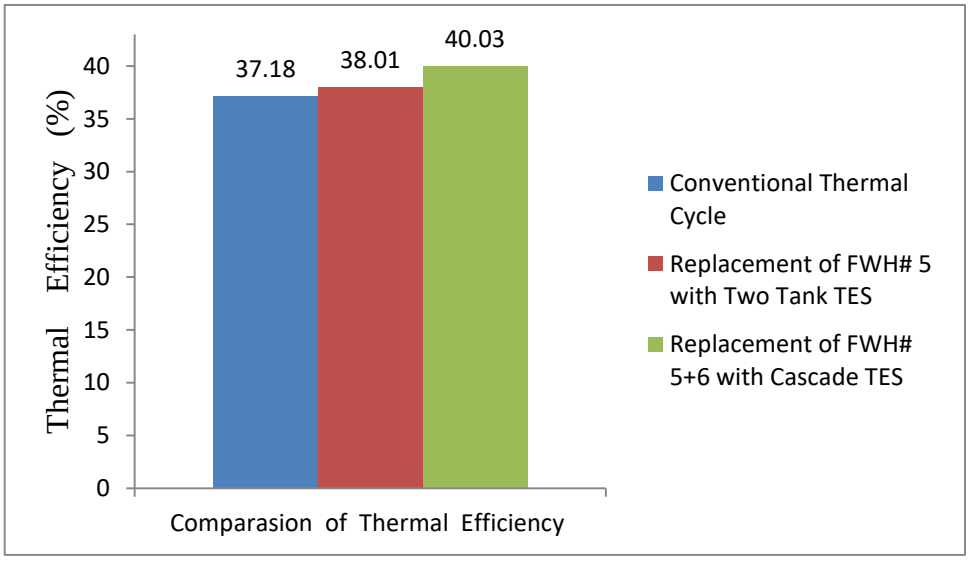

Fig. 13. Comparison of the Efficiency of SITC with Different TES

4.7.4. Comparison of Fuel Saving in SITC with TES

Due to the availability of additional solar energy as a heat source in the thermal power cycle, the coal requirement decreases. Coal consumption rate decreases with the available energy. Due to the decrease in coal consumption, the fuel saving rate improves. It is already discussed that two tank TES stores less energy as compared to the cascade TES. So, coal consumption rate is high and the fuel saving rate is low as compared to cascade TES.

Figure 14 presents a comparison of coal consumption and fuel saving rates for the two-tank and cascade TES systems. The fuel saving rate is 5.40 kg/s for the cascade TES, compared to 4.58 kg/s for the two-tank TES. The corresponding coal consumption rate is 37.34 kg/s with the cascade TES, which is lower than that of the two-tank TES (38.14 kg/s).

4.7.5. Comparison of CO_2 Emission

With the integration of TES with SITC, different performance parameters improve such as saving of Thermal energy and fuel saving, cycle efficiency etc. In a conventional power cycle coal is use as fuel, which causes CO_2 emissions. It is a major problem of the thermal power cycle because it affects the environment.

Power utilities are increasingly focusing on technologies that reduce CO_2 emissions, including the integration of renewable energy sources for power generation. In the present study, the solar cycle is integrated with a conventional thermal power cycle, leading to a reduction in coal consumption and a corresponding decrease in CO_2 emissions. .ion in CO_2 emissions per annum with the use of different types of TES.

5. Validation

The thermodynamic modelling of a cascade thermal storage system was developed by using MATLAB in the present study. Different parameters are considered to validate the simulation results obtained by the proposed model. The Fig. 16 shows the comparison of simulated parameters and the designed value.

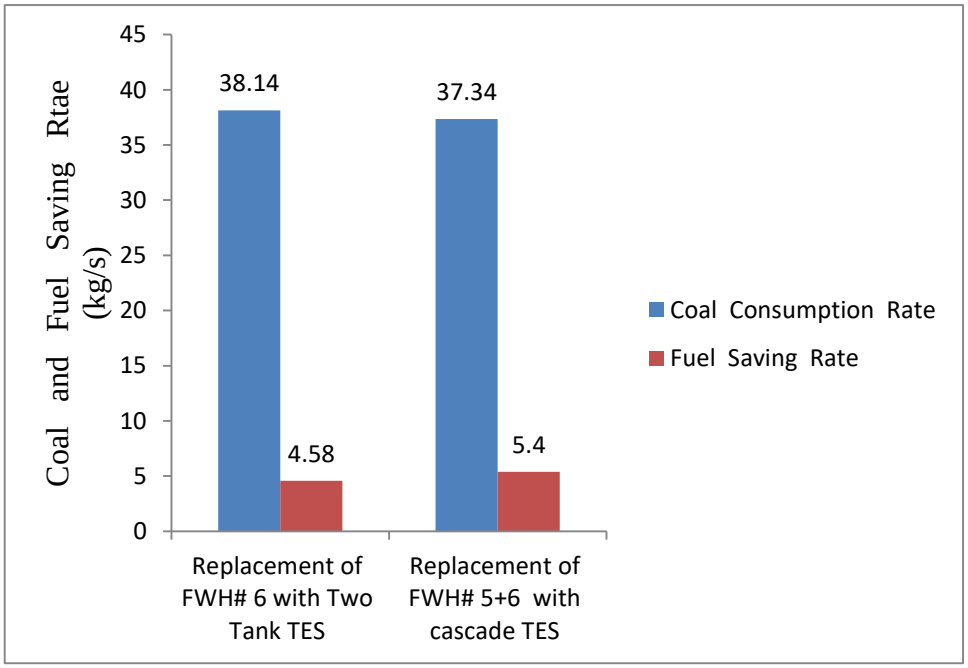

Fig. 14. Comparasion of Coal Consumption rate and Fuel Saving in SITC With Different TES.

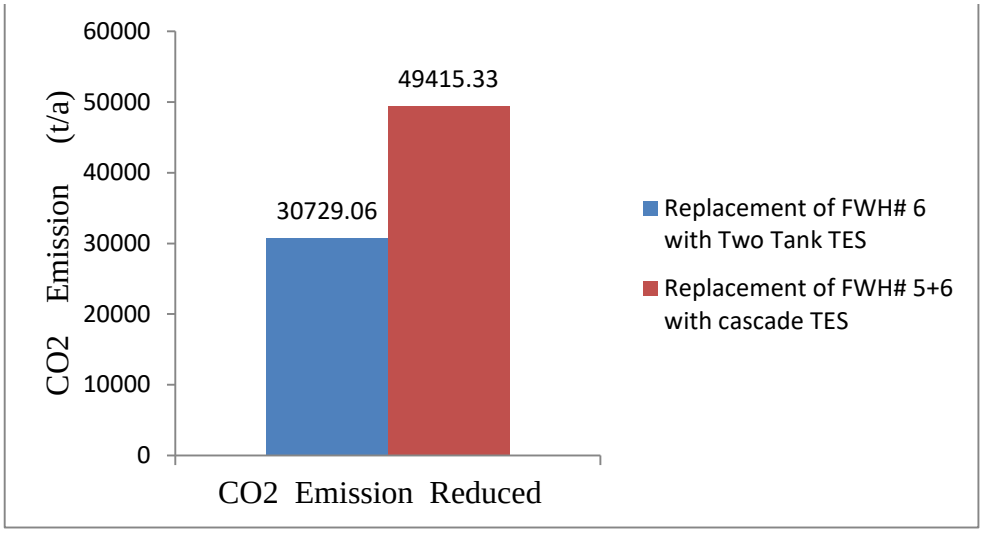

Fig. 15. Comparison of CO_2 Emission with Different TES

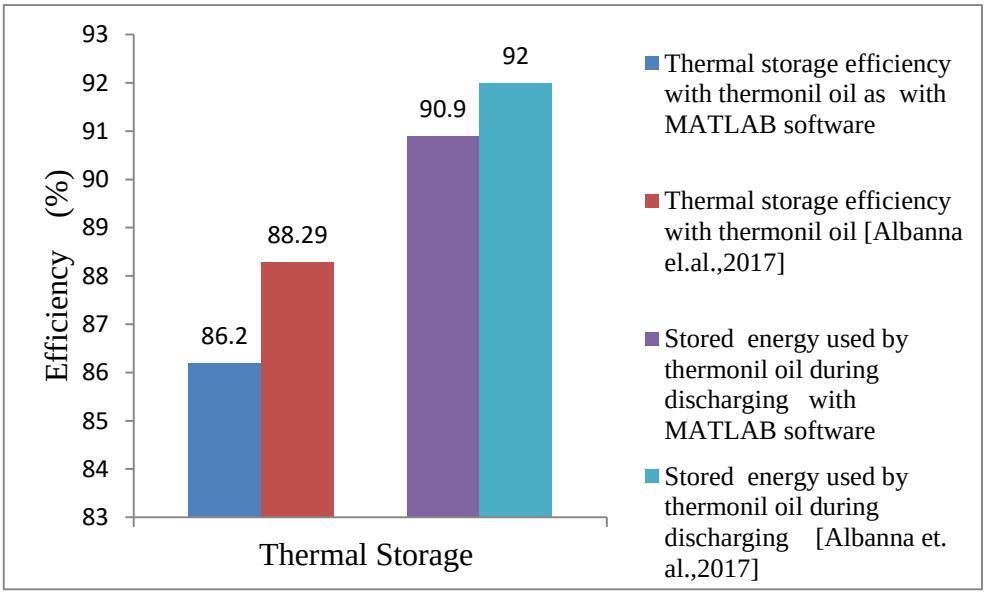

Fig. 16. Validation for Different Performance of Cascade Thermal storage With Referred Literature

6. Conclusions

The work presents the impact of thermal storage integration with a concentrated solar system for utilising the solar energy even during non-solar hours. In the present work the LFR solar system is integrated with the Two tank and Cascade thermal storage and a thermodynamic model of the system has been developed. The mathematical model with MATLAB coding has been developed to simulate the performance of thermal storage for various parametric variations. Based upon the performance analysis, the major conclusions are drawn as follows.

1. The mass flow rate of HTF in the solar receiver is dependent of DNI which varies with weather and type of HTF used in the receiver. It is 150.45 kg/s, 143.35 kg/s, 138.1 kg/s and 100.36 kg/s in Summer, Autumn, Spring, and Winter respectively with Molten salt which is less than oil.
2. The temperature difference in the TES varies with the use of different HTFs. The difference in temperature is more when HTF enters with more temperature in TES during charging process. Molten salt is entered in the tank at 525 °C while with oil is 385°C. So, the temperature

difference exist in TES with molten salt is more as compared to Therminol oil and that is 260 °C for average DNI of 550 W/m^2.

3. During the charging process, PCM starts to melt, and energy is stored in TES for further use. The stored energy in TES depends on HTF used in the solar receiver. The stored energy is 36.75 MW with molten salt and 28.18 MW with oil. The stored energy is more with molten salt as compared to other TES as because of its high temperature limits, four layers of PCM can be possible in a thermal storage system with molten salt.
4. Thermal storage efficiency is dependent on the energy stored, and the energy stored is more with molten salt than Therminol oil. The storage tank efficiency is possible up to 80.57% with molten salt, which is higher by 3.37% and 9.03 % as compared to cascade TES (Therminol oil) and Two tank TES.
5. The discharging temperature plays a vital role for further use of this HTF for any further applications because of its associated heat. The discharging temperature is 350°C and 501 °C with Therminol oil and molten salt, respectively.
6. The discharging temperature of HTF is dependent on the amount of stored energy by HTF. It is possible to use 92% of the stored energy with oil and 95.5% with molten salt. The molten salt absorbs more stored energy and therefore improves the temperature of HTF during the discharging period and provides more energy for further use.
7. Efficiency of ISTC increases with the integration of TES. It increases by 0.83 % with two tank TES, while 2.85% with cascade TES (Molten salt as HTF).
8. Coal consumption rate and CO_2 emission further decrease with cascade TES as compared to two tank TES. The coal consumption rate is 37.34 kg/s with cascade TES (Molten salt), which is less than Two tank TES.
1. Further, the CO_2 emission is 49415.33 (t /a) with cascade TES, while it is 30729.06 (t/a) for Two tank TES. Hence, this integration contributes to saving the environment.

References

[1] Achour, L., Bouharkat, M. and Behar, O., 2018. Performance assessment of an integrated solar combined cycle in the southern of Algeria. Energy Reports, 4, 207-217. (https://doi.org/10.1016/j.egyr.2017.09.003

[2] Albanna, M. I., Altamimi, N. K., &Abuhamra, R. A. Design of Heat Exchanger for Thermal Energy Storage Using High Temperature Phase Change Material ﻫُ

[3] Alva, G., Liu, L., Huang, X., & Fang, G. 2017. Thermal energy storage materials and systems for solar energy applications. Renewable and Sustainable Energy Reviews, 68, 693-706. (https://doi.org/10.1016/j.rser.2016.10.021)

[4] Amano, R.S., Abbas, A., 2017. Integration of Linear Fresnel Reflectors (LFR) with Conventional Power Plants. In 15th International Energy Conversion Engineering Conference , 4624. (https://doi.org/10.2514/6.2017-4624).

[5] Antonanzas, J., Alia-Martinez, M., Martinez-de-Pison, F. J., & Antonanzas-Torres, F. (2015). Towards the hybridization of gas-fired power plants: a case study of Algeria. Renewable and Sustainable Energy Reviews, 51, 116-124.https://doi.org/10.1016/j.rser.2015.06.019

[6] Beghi C., Thermal energy storage. Dordrect, Holland: D. Reidel Publication Co, 2015.

[7] Da Cunha, J. P., & Eames, P., 2016. Thermal energy storage for low and medium temperature applications using phase change materials–a review. Applied Energy, 177, 227-238 (https://doi.org/10.1016/j.apenergy.2016.05.097)

[8] Desai, N.B., and Bandyopadhyay, S., 2015. Optimization of concentrating solar thermal power plant based on parabolic trough collector. Journal of Cleaner Production, 89, 262-271 (https://doi.org/10.1016/j.jclepro.2014.10.097

[9] Duffie, J.A. and Beckman, W.A., 2013. Solar engineering of thermal processes. John Wiley &Sons.ISBN 978-0-470-87366-3

[10] El Gharbi, N., Derbal, H., Bouaichaoui, S., & Said, N. 2011. A comparative study between parabolic trough collector and linear Fresnel reflector technologies. Energy Procedia, 6, 565-572. https://doi.org/10.1016/j.egypro.2011.05.065

[11] Elfeky, K. E., Mohammed, A. G., Ahmed, N., Lu, L., & Wang, Q., 2020. Thermal and economic evaluation of phase change material volume fraction for thermocline tank used in concentrating solar power plants. Applied Energy, 267, 115054.(https://doi.org/10.1016/j.apenergy.2020.115054)

[12] Garg H.P., Mullick S.C., Bhargava V.K., Solar thermal energy storage. Springer Science & Business Media, 2012

[13] Khandelwal, N., Sharma, M., Singh, O., & Shukla, A. K. (2020). Recent developments in integrated solar combined cycle power plants. Journal of Thermal Science, 29(2), 298-322.https://doi.org/10.1007/s11630-020-1278-2

[14] Khandelwal, N., Sharma, M., Singh, O., & Shukla, A. K. (2020). Comparative analysis of the linear Fresnel reflector assisted solar cycle on the basis of heat transfer fluids. Materials Today: Proceedings.(https://doi.org/10.1016/j.matpr.2020.05.792)

[15] Khandelwal, N., Sharma, M., Singh, O., & Shukla, A. K., 2021. Thermo-economic analysis of an integrated solar thermal cycle (ISTC) using thermal storage. Journal of Cleaner Production, 128725.DOI: 10.1016/j.jclepro.2021.128725

[16] Khandelwal, N., Sharma, M., Singh, O., & Shukla, A. K. 2022. Comparative evaluation of Integrated Solar combined cycle plant with cascade thermal storage system for different heat transfer fluids. Journal of Cleaner Production, 131519. https://doi.org/10.1016/j.jclepro.2022.131519

[17] Kumar, R., 2017. A critical review on energy, exergy, exergoeconomic and economic (4-E) analysis of thermal power plants. Engineering Science and Technology, an International Journal, 20(1),283-292. (https://doi.org/10.1016/j.jestch.2016.08.018)

[18] Kumar, R., Sharma, A.K., Tewari, P.C., 2014. Thermal performance and economic analysis of 210 MWe coal-fired power plant. Journal of Thermodynamics. (http://dx.doi.org/10.1155/2014/520183

[19] Müller-Steinhagen, H., Trieb, F., Concentrating solar power. A review of the technology. Ingenia Inform QR AcadEng, 2004, 18: 43–50.

[20] Mokheimer, E.M., Dabwan, Y.N., Habib, M.A., Said, S.A., and Al-Sulaiman, F.A., 2014. Techno-economic performance analysis of parabolic trough collector in Dhahran, Saudi Arabia. Energy conversion and management, 86, 622-633.(https://doi.org/10.1016/j.enconman.2014.06.023)

[21] Modi, A., & Haglind, F. (2014). Performance analysis of a Kalina cycle for a central receiver solar thermal power plant with direct steam generation. Applied Thermal Engineering, 65(1-2), 20208.https://doi.org/10.1016/j.applthermaleng.2014.01.010

[22] Khandelwal, N., Sharma, M., Singh, O., & Shukla, A. K. (2022, February). Comparative investigation on two tank and cascade thermal storage for solar power plants. In Journal of Physics: Conference Series (Vol. 2178, No. 1, p. 012013). IOP Publishing.

[23] Pacio, J., & Wetzel, T. (2013). Assessment of liquid metal technology status and research paths for their use as efficient heat transfer fluids in solar central receiver systems. Solar Energy, 93, 11-22.https://doi.org/10.1016/j.solener.2013.03.025

[24] Pelay U., Luo L., Fan Y., Stito D., Rood M., et al., Thermal energy storage systems for concentrated solar power plants. Renewable and Sustainable Energy Reviews, 2017, 7: 82–100.DOI: 10.1016/j.rser.2017.03.139

[25] Peterseim, J. H., White, S., Tadros, A., & Hellwig, U. (2013). Concentrated solar

power hybrid plants, which technologies are best suited for hybridisation?. Renewable Energy, 57, 520-532.https://doi.org/10.1016/j.renene.2013.02.014

[26] P.Kurup, T. Kwasnik, B.J. Roberts, and T. Wendelin, " Initial thermal energy yield potential for the use of concentrating solar power (CSP) for coal hybridization in India (No. NREL/TP-6A20-74024)," National Renewable Energy Lab.(NREL), Golden, CO (United States

[27] Prasad JS, Muthukumar P, Anandalakshmi R, Niyas H.,2018 Comparative study of phase change phenomenon in high temperature cascade latent heat energy storage system using conduction and conduction-convection models. Sol Energy ,176:627–37.(https://doi.org/10.1016/j.solener.2018.10.048)

[28] Rongrong, Z., Yongping, Y., Qin, Y., & Yong, Z. (2013). Modeling and characteristic analysis of a solar parabolic trough system: thermal oil as the heat transfer fluid. Journal of Renewable Energy, 2013.https://doi.org/10.1155/2013/389514

[29] Tian Y., Zhao C.Y., A review of solar collectors and thermal energy storage in solar thermal applications. Applied Energy, 2012, 104: 538–553. https://doi.org/10.1016/j.apenergy.2012.11.051

[30] Vignarooban K., Xu X., Arvay A., Hsu K., Kannan A.M.,2015 Heat transfer fluids for concentrating solar power systems–a review. Applied Energy, 146: 383–396(https://doi.org/10.1016/j.apenergy.2015.01.125)

[31] Wei, G., Wang, G., Xu, C., Ju, X., Xing, L., Du, X., & Yang, Y. 2018. Selection principles and thermophysical properties of high temperature phase change materials for thermal energy storage: A review. Renewable and Sustainable Energy Reviews, 81, 1771-1786. (DOI: 10.1016/j.rser.2017.05.271)

[32] Sharma, M., Shukla, A.K., Singh, A., Johri, S. and Singh, H.P., 2020. Parametric analysis of solar energy conversion system using parabolic concentrator and thermopile. International Journal of Ambient Energy, 41(12), pp.1409-1414. (https://doi.org/10.1080/01430750.2018.1517672)

[33] Vir, A., (2012). Solar Booster Augmentation for Existing Coal Fired Power Plant (A Feasibility Study).https://www.divaportal.org/smash/get/diva2:562376/FULLTEXT01.pd

[34] Tay, N. H. S., Belusko, M., & Bruno, F.,2012. Designing a PCM storage system using the effectiveness-number of transfer units method in low energy cooling of buildings. Energy and buildings, 50,234242.https://doi.org/10.1016/j.enbuild.2012.03.041